Formulation of Turbulent Fluxes in the Stable Boundary Layer

L. MAHRT AND DEAN VICKERS

College of Oceanic and Atmospheric Sciences, Oregon State University, Corvallis, Oregon

(Manuscript received 20 June 2002, in final form 13 January 2003)

ABSTRACT

The mixing lengths for heat and momentum are computed from seven levels of eddy correlation data during the Cooperative Atmosphere–Surface Exchange Study-1999 (CASES-99). A number of formulations of the mixing length are evaluated, including surface layer similarity theory, several hybrid similarity theories, a formulation based on the Richardson number, and a formulation based on the local shear. A formulation of the mixing length is examined, which approaches *z*-less similarity for large *z* and surface layer similarity close to the ground surface. A generalized version includes a dependence on boundary layer depth, which approaches the usual boundary layer height dependence for neutral conditions. However, for many of the observational cases, a boundary layer did not exist in the usual sense, in that turbulence was generated primarily above the surface inversion layer and occasionally extended downward toward the surface. For these cases, inclusion of *z*-less turbulence is crucial.

1. Introduction

Existing models of the stable boundary layer perform reasonably well in many situations but fail in some common situations. For example, the boundary layer depth is often not definable in situations where the turbulence is generated primarily by shear above the surface inversion layer and then diffuses downward toward the surface. Misrepresentation of such influences and underprediction of mixing in models may be one of several effects causing overprediction of surface cooling (Delage et al. 2002). Most numerical models of the stable boundary layer require definition of the boundary layer depth as a fundamental cornerstone of the parameterization, either in terms of eddy diffusivity profile functions or as one of the length scales in the parameterization of the mixing length.

Boundary layers are difficult to define when the principal source of turbulence is shear generation of turbulence semidetached from the surface (Smedman et al. 1993; Mahrt and Vickers 2002), sometimes occurring at the top of the surface inversion layer. Such shear generation could be associated with enhancement of shear by the nocturnal low-level jet (e.g., Blackadar 1957; Ostdiek and Blumen 1997), modulation of shear by internal gravity waves (Chimonas 2002), acceleration associated with decoupling (Derbyshire 1999) or generation of turbulence associated with unstable waves and density currents (Sun et al. 2003). In these cases, shear-generated turbulence may intermittently burst downward toward the surface (Nappo 1991; Ohya 2001; Cuxart et al. 2000). This situation has been referred to as the upside-down boundary layer by Mahrt (1999) and others, although this usage of the term boundary layer does not satisfy traditional boundary layer concepts. We postpone introduction of additional terminology until the physics is better understood. The literature contains a number of multilayer conceptual models of the nocturnal ''boundary layer'' (e.g., Beyrich 1997), although different studies emphasize different variables and are difficult to intercompare.

The region of generation of turbulence at higher levels occurs in what is normally referred to as the ''residual layer.'' We find this term too passive in that the turbulence is actively generated by shear associated with nocturnal flow accelerations. Perhaps ''*z*-less'' layer is a more suitable term. Here *z*-less turbulence (Wyngaard 1973) does not scale with height above the ground nor the boundary layer depth. The present study indicates that *z*-less conditions are more prevalent than previously thought, even in a relatively windy environment.

An additional modeling difficulty is that the nocturnal boundary layer may be extremely thin, less than 10 m deep (Smedman 1988). Models generally do not employ sufficient vertical resolution to resolve very thin stable boundary layers. In the worst scenario, the boundary layer is so shallow that a surface layer does not exist; that is, the roughness sublayer (Raupach 1994; additional references in Mahrt 1999) occupies more than the lowest 10% or 20% of the boundary layer. In this case, Monin–Obukhov theory does not apply at any level.

Corresponding author address: Dr. Larry Mahrt, College of Oceanic and Atmospheric Sciences, Oregon State University, 104 Ocean Adm. Building, Corvallis, OR 97331-5503.
E-mail: mahrt@coas.oregonstate.edu

Based on eddy correlation data at seven levels on a 60-m tower, this study constructs a general formulation of the mixing length that includes cases where the boundary layer is not definable.

2. Data

The dataset includes six levels of sonic anemometer data from the 60-m tower in the Cooperative Atmosphere–Surface Exchange Study-1999 (CASES-99; Poulos et al. 2002). In addition, we include data from the 1.5- and 5-m levels on a minitower, 10 m to the side of the main tower. The data have been quality controlled using an improved version of Vickers and Mahrt (1997). The number of complete vertical profiles is reduced to 160 h, mainly due to missing data at the 10- and 20-m levels and to elimination of cases with airflow through the tower prior to reaching the eddy correlation sensors. The fluxes are computed from a height- and stability-dependent averaging length for computing perturbation quantities (Vickers and Mahrt 2003), which decreases from a height-dependent value of greater than 500 s at neutral conditions to a minimum value of 30 s for very stable conditions. The decreasing window width recognizes the decreasing scale of turbulent transport with increasing stability and proximity to the ground surface and attempts to minimize the influence of mesoscale motions on the computed perturbation quantities. Fluxes are then averaged over 1-h periods to reduce random flux sampling errors.

The mean shear is computed using the propeller anemometer and wind vane data for 15 m and above, and also uses the sonic anemometers at 5 and 1.5 m. Profiles of potential temperature on the main tower are computed from aspirated shielded thermistors at 5, 15, 25, 35, 45, and 55 m. The gradients are computed from simple finite differencing, which sometimes led to rapid variation with height and contributed to the scatter in various relationships examined in this study. The Richardson number was computed from the gradients of potential temperature and wind as computed above. The calculation of the nondimensional gradient of potential temperature for near-neutral conditions is problematic, partly because the number of near-neutral cases is small and estimation of the weak heat flux and weak vertical gradient of potential temperature in near-neutral conditions is vulnerable to error. This is especially true near the surface where the resolution of the vertical gradient is poor, and we are forced to use the surface radiation temperature for the lower boundary condition. The surface radiation is computed from an average of the five values measured in a network about the tower (Burns et al. 2003).

For this analysis, very stable cases are excluded ($z/L > 2$) where relative flux sampling errors are often large. The fit for the nondimensional gradients (section 3) is confined to the range 0–20. To compute the bin-averaged ratios, the numerator and the denominator are averaged first to avoid the ratio averaging problem where very large ratios occur for a few records due to very small fluxes in the denominator.

Close to the surface, where part of the flux can be carried by eddies not resolved by the sonic anemometers, the flux may be underestimated. Unfortunately, in thin stable boundary layers, the flux must be measured very close to the surface in order to remain in the surface layer where Monin–Obukhov similarity theory is valid. Both flux loss due to pathlength averaging by the sonic anemometer and vertical flux divergence between the surface and observational level may cause the surface flux to be incorrectly estimated.

The boundary layer depth is estimated from profiles of the buoyancy flux with consideration of the profiles of the momentum flux and vertical velocity variance. The boundary layer depth is more easily defined in terms of the buoyancy flux because the small stratification above the surface inversion layer often forces the buoyancy flux to small values even when the turbulence energy and momentum flux do not decrease with height. In this sense, the height dependence of the buoyancy flux is more regular than that for the turbulence energy and momentum flux. Even so, the buoyancy flux still increases with height for part or all of the tower layer in many cases due to near-collapsed turbulence close to the surface and significant turbulence at higher levels with some stratification. The boundary layer depth based on the 160 buoyancy flux profiles, where data are available at all levels, is subjectively estimated as top of the layer where the buoyancy flux decreases monotonically with height and approximately vanishes. The buoyancy flux profiles are categorized as

1) 44 cases where the buoyancy flux decreases with height to small values and then remains relatively small at higher levels in the tower layer, allowing relatively clear definition of the boundary layer depth in terms of the buoyancy flux;
2) 40 cases where a boundary layer depth is definable but the buoyancy flux does not remain small above the boundary layer;
3) 86 cases where the turbulence generally increases with height across the tower layer, although some of these cases may include a very shallow layer near the surface where the buoyancy flux decreases with height, belonging to class 2 as well;
4) 6 cases where the buoyancy flux was relatively independent of height, implying a deep boundary layer, and 7 cases where the buoyancy flux varied erratically with height, sometimes corresponding to layering.

Thus, a traditional boundary layer could be defined only about 25% of the time, and even less often when posed in terms of the momentum flux or turbulence energy. The buoyancy flux increased with height for a significant fraction of the tower layer for approximately 53% of the cases.

Several of the relationships examined in this study are subjected to self-correlation (e.g., Hicks 1978). For example, the mixing length is proportional to the square root of the stress (local friction velocity) while several of the models of the mixing length contain the friction velocity, guaranteeing some correlation even for purely random data. As one measure of the self-correlation, we randomly redistribute the observed values of the friction velocity, heat flux, wind speed, wind shear, and potential temperature gradient. This process is carried out by assigning a record number to each of the N records. The friction velocity for the first new random record is extracted from an original record chosen at random. This process is carried out for each variable until a new random record is determined. Then the mixing length is computed from the friction velocity and wind shear for this random record. This process is repeated until a set of N new random records are constructed. For the new random records, we compute the mixing length from the randomized data for each of the N records and then compute the variance explained by the various mixing-length formulations for the N records. This entire process is repeated for 1000 realizations and then the variance explained is averaged over all of the realizations.

3. Flux formulation

Turbulent transport within the stable boundary layer is often parameterized in terms of a stability-dependent mixing length or eddy diffusivity. This approach assumes that the flux is related to the local vertical gradient. Such parameterizations have not been rigorously compared with eddy covariance measurements above the surface layer in the stable boundary layer. They have been evaluated more indirectly in terms of overall model performance.

The turbulent momentum flux for the u component can be written as

$$\overline{w'u'} = -K_m\left(\frac{z}{h}\right)\frac{\partial \overline{u}}{\partial z}. \tag{1}$$

A similar expression is written for the v component. Using Brost and Wyngaard (1978) and matching with surface layer scaling, Troen and Mahrt (1986) derived a formulation for the eddy diffusivity as

$$K_m = \frac{u_*}{\phi_m}\left(\frac{z}{L}\right)h\kappa\frac{z}{h}\left(1 - \frac{z}{h}\right)^p, \tag{2}$$

where $p = 2.0$ and u_* and L are computed from surface fluxes and the nondimensional shear ϕ_m is defined as

$$\phi_m\left(\frac{z}{L}\right) \equiv \frac{\kappa z}{u_*}\frac{\partial \overline{u}}{\partial z}, \tag{3}$$

where L is the Obukhov length (Monin and Obukhov 1954) and κ is von Kármán's constant. For stable conditions, the nondimensional shear is often approximated as (Dyer 1974)

$$\phi_m(z/L) = 1 + \beta z/L. \tag{4}$$

The Monin–Obukhov similarity theory assumes that the stress, mean wind, and mean wind shear vectors are all aligned.

With the traditional derivation of the mixing length formulation (normally accredited to Prandtl; see Arya 1998), one assumes that velocity perturbations are induced by vertical movement of fluid elements in a shear flow such that the magnitude of the velocity fluctuation is approximated as

$$V' \approx l\frac{\partial \overline{u}}{\partial z}, \tag{5}$$

where l is the vertical displacement of the fluid element, V' is a velocity scale for the horizontal velocity fluctuations and the u direction is locally aligned to the wind shear for this derivation. This derivation assumes that the momentum of the fluid element is conserved during the displacement in an environment with no mean directional shear, which, in turn, assumes that the fluid element is not influenced by mixing with the flow around it, nor influenced by pressure perturbations. Both processes would normally reduce V'. This formulation also assumes that the shear is constant with height. With height-dependent shear, one would need to more carefully evaluate the gradient on the scale of the mixing length itself.

Neglecting the difference between the horizontal and vertical scale of the eddies, the incompressible mass continuity equation scales as

$$\frac{w'}{l} \approx -\frac{V'}{l}. \tag{6}$$

From Eqs. (1), (5), and (6), one traditionally derives the eddy diffusivity for momentum as

$$K_m = l^2\left(\frac{\partial \overline{u}}{\partial z}\right), \tag{7}$$

which formally defines the mixing length. Gradients are assumed to be positive or replaced with the absolute value. Slightly different derivations can be found in Stull (1990) and Arya (1998). Alternatively, one can obtain the same relationship by defining the mixing length in terms of dimensional considerations to be

$$l \equiv \frac{u_*}{\partial \overline{u}/\partial z}. \tag{8}$$

Allowing for the difference between mixing of momentum and scalars, the perturbation of the scalar, such as potential temperature, is written as

$$\theta' \approx l_h\frac{\partial \overline{\theta}}{\partial z}, \tag{9}$$

where l_h is the scalar mixing length. Combining Eqs. (5), (6), and (9), the heat flux is estimated as

$$\overline{w'\theta'} = -l_h l \frac{\partial \overline{\theta}}{\partial z}\left(\frac{\partial \overline{u}}{\partial z}\right), \tag{10}$$

in which case the eddy diffusivity for heat becomes

$$K_h = l_h l \frac{\partial \overline{u}}{\partial z}. \tag{11}$$

The observed mixing length for heat behaves significantly differently than that for momentum (section 7).

a. Mixing-length formulations

Generally, mixing-length formulations do not distinguish between momentum and scalar transport. A common early formulation for the mixing length (Blackadar 1962) is written as

$$l = \frac{\kappa z}{1 + \kappa z/\lambda_B}, \tag{12}$$

where λ_B is an adjustable length scale. Ballard et al. (1991) specifies λ_B to be one-third of the boundary layer depth. They use this value above the boundary layer as well.

A variety of mixing-length schemes have been derived that allow more flexibility than the original Blackadar scheme and in particular include the influence of stability and approach Monin–Obukhov similarity theory at the surface. These schemes (e.g., Therry and Lacarrere 1983; Ballard et al. 1991) still include the Blackadar formulation as one of the functional dependencies but are generally too complex to directly evaluate from existing data. Alternatively, Eq. (12) can be generalized to include a dependency on Richardson number (Savijärvi and Kauhanen 2002).

When the boundary layer is well defined, the mixing length can alternatively be expressed in the format

$$l = \frac{\kappa z}{\phi_m}\left(1 - \frac{z}{h}\right)^p, \tag{13}$$

where p is a nondimensional coefficient. This relationship approaches surface layer similarity value for small z/h, reaches a maximum in the interior, and vanishes at the boundary layer top. Although similar, this approach is not equivalent to the mixing length that can be derived from the boundary layer formulation of the eddy diffusivity [Eq. (2)]. With these two relationships, both the eddy diffusivity and the mixing length are predicted to increase with increasing boundary layer depth. The mixing-length formulations considered in this study are summarized in Table 1.

TABLE 1. Mixing-length formulations not requiring boundary layer depth.

Formulation	Equation	Evaluation
Blackadar (1692)	(12)	
Hybrid.	(17)	Sections 4, 5; Figs. 2, 3
Garratt (1992)	(21)	
Kim and Mahrt (1992)	(22)	
Shear length	(23)	Sections 2, 6; Fig. 2
B.V.-w	(24)	Sections 2, 6; Fig. 2
B.V.-u_*	(30)	Sections 2, 6; Fig. 2

b. z-less vertical mixing based on hybrid similarity

For very stable conditions, the height above ground and the boundary layer depth may no longer be relevant scaling variables. Zilitinkevich and Mironov (1996) derive a limiting Richardson number as a form of z-less turbulence [limiting case of their Eq. (10)]. With this approach, the mean shear becomes proportional to the Brunt–Väisälä frequency with strong stratification, corresponding to height-independent Richardson number. The log-linear law for the nondimensional shear [Eq. (4)] becomes independent of z in the limit of large z/L (e.g., Sorbjan 1989, section 4.2.3; Monin and Yaglom 1971). For very stable conditions ($z/L \gg 1$), the second term on the right-hand side of the expression for the nondimensional shear [Eq. (4)] dominates. Then, Eqs. (3)–(4) lead to the z-less asymptotic limit

$$u_*(z) = L\frac{\kappa}{\beta}\frac{\partial \overline{u}}{\partial z}, \tag{14}$$

where the Obukhov length and friction velocity are now computed from local values of fluxes at level z, in which case the Obukhov length is usually symbolized as λ. Then the mixing length becomes

$$l = \lambda\frac{\kappa}{\beta}, \tag{15}$$

where κ/β is order of 10^{-1}. This is one of the terms in the mixing-length formulation of Delage (1974). As z approaches the surface λ approaches L. In actuality, most observational investigations of similarity in the stable boundary layer are, sometimes unknowingly, posed in terms of λ because the surface layer is often below standard observational levels for strong stability, such as 2 or 10 m, at least for the present dataset (section 5). That is, the fluxes at the standard observational levels are different from the surface fluxes. In fact, a surface layer may not even exist for some stable boundary layers, as noted in the introduction.

Since the fluxes at level z may not be equal to the surface fluxes, we must replace the surface layer nondimensional shear with a ''hybrid'' nondimensional shear:

$$\Phi_m\left(\frac{z}{\lambda}\right) \equiv \frac{\kappa z}{u_*(z)}\frac{\partial \overline{u}}{\partial z}. \tag{16}$$

Then, the similarity prediction of the mixing length can be expressed as

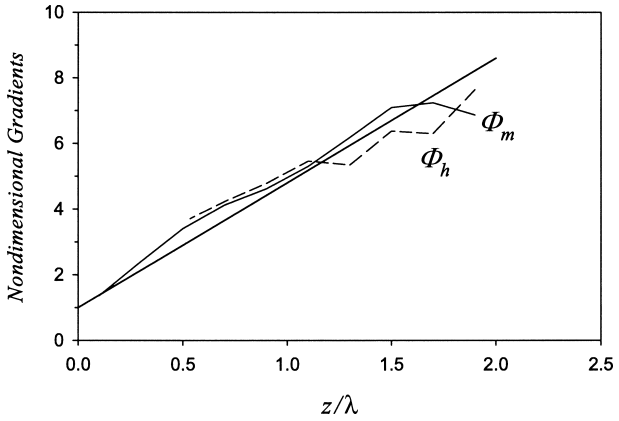

FIG. 1. Bin-averaged Φ_m and Φ_h as a function of z/λ based on local fluxes at level z for all levels combined. The solid line is $1 + 3.7\ z/\lambda$.

$$\frac{\kappa z}{\Phi_m}, \tag{17}$$

where

$$\Phi_m(z/\lambda) = 1 + \beta z/\lambda. \tag{18}$$

We will refer to Eq. (18) as hybrid similarity theory since it approaches Monin–Obukhov similarity theory as z approaches the surface and approaches z-less similarity theory as z becomes sufficiently large. Hybrid similarity theory is not as rigorous as matching boundary layer similarity theory with surface similarity theory, but it is simpler and more practical, does not require definition of a boundary layer depth, and performs quite well (section 4). Equation (18) is not equivalent to ''local similarity'' theory, as will be discussed below.

Based on the CASES-99 data, the best fit of the data to Eq. (18) is obtained with $\beta = 3.7$ as shown in Fig. 1. Here, the observed mixing length is bin averaged according to intervals of z/λ. Note that Φ_m asymptotes to near unity as z/λ approaches zero. The value of $\beta = 3.7$ is smaller than those reported in the literature (Högström 1996) for Monin–Obukhov similarity theory ($\lambda \rightarrow L$). A fit to the present data for small z/λ below 10 m yields higher values of β; the exact value depends on the stability range included in the analysis. The values of Φ_m for $z/\lambda > 1.5$ are overestimated by the linear model (Fig. 1). That is, Φ_m increases a little more slowly than linear for large stability, as found in previous studies (Beljaars and Holtslag 1991; Garratt 1992, p. 52; Vickers and Mahrt 1999). Here, we still employ the linear version in order to include the z-less asymptote. For $z/\lambda > 2$ (not shown), the scatter continues to increase with increasing z/λ, suggesting observational difficulties and/or inapplicability of similarity theory. The values of the nondimensional gradient of potential temperature for the present data are often not trustworthy for near-neutral conditions (section 2) and are omitted in Fig. 1 for $z/\lambda < 0.5$.

c. Local similarity

In local similarity theory, λ replaces height above ground in the definition of the nondimensional shear such that (Nieuwstadt 1984)

$$\Phi'_m \equiv \frac{\kappa\lambda}{u_*(z)}\frac{\partial \overline{u}}{\partial z}. \tag{19}$$

Sorbjan (1986) concisely summarizes local similarity theory as consisting of three hypotheses: 1) scaling arguments can be constructed in terms of local fluxes at level z, 2) the nondimensional shear Φ'_m can be expressed as a function of z/λ and that those functions can be approximated by the same mathematical form as those in Monin–Obukhov similarity theory, and 3) the height dependence of the fluxes can be modeled in terms of z/h. Hypotheses 2 and 3 introduce the height above ground and the boundary layer depth as scaling variables so that the ''local'' similarity theory is not purely local. This set of conditions is quite different from z-less similarity where height above the ground and the boundary layer depth are not relevant length scales.

The nondimensional shear for local similarity theory [Eq. (19)] does not analytically lead to a z-less asymptotic limit as z/λ approaches large values, in contrast to the asymptotic limit for Monin–Obukhov similarity theory [Eq. (14)]. However, Sorbjan (1988) has noted that the nondimensional gradients for local similarity theory computed from eddy correlation data do indeed approach constants for z/λ greater than about 5, although the asymptotic value of Φ'_m varies between studies, apparently due to other complications such as sloped terrain (Sorbjan 1988).

The relationship between Φ'_m and z/λ is difficult to evaluate from data because both functions contain λ and the statistical relationship between them can be dominated by self-correlation (section 2) for the data in this study. For this reason, local similarity theory is not evaluated further.

d. Other z-less formulations

A general z-less formulation of the mixing length can be developed in terms of the local gradient Richardson number

$$l = f(\mathrm{Ri}). \tag{20}$$

Garratt (1992, p. 246) presents a typical format of the mixing length in meters to be

$$l = \frac{1}{(1 + c\mathrm{Ri})^2}, \tag{21}$$

where c is considered to be different for momentum transfer and scalar transfer, although specific values of c are not given.

Kim and Mahrt (1992) recommend the formulation

$$l = l_0\left[\exp(-c_1\mathrm{Ri}) + \frac{c_2}{\mathrm{Ri} + c_3}\right]. \quad (22)$$

With the coefficients (c_1, c_2, c_3) specified in Kim and Mahrt (1992), the mixing length decreases from slightly greater than the asymptotic mixing length (l_0) at neutral stability (Ri = 0) to vanishingly small values at large Ri. Although the above formulation was fit to eddy correlation data, Ha and Mahrt (2001) found that l_0 in Eq. (22) had to be reduced from 50 to 15 m in order to improve the overall performance of their boundary layer scheme. It is not known if this reduction of the asymptotic mixing length is due to compensation for other inadequacies in their model or if the empirical formulation was biased.

The bulk potential temperature and velocity gradients can be directly converted to a shear length scale with the formulation

$$l = S \equiv C(z, \Delta z)\frac{(\Delta U)^2}{(g/\Theta)\Delta\Theta}, \quad (23)$$

where $C(z, \Delta z)$ is a nondimensional coefficient, which, for a fixed z and Δz, is inversely proportional to the Richardson number. This formulation avoids specification of the neutral asymptotic length scale but is truly z-less only if $C(z, \Delta z)$ becomes independent of height.

Another simple formulation of the mixing length for z-less conditions can be derived from scale analysis or parcel theory as

$$l = C_{\mathrm{BV}}\frac{\sigma_w}{N}, \quad (24)$$

where N is the Brunt–Väisälä frequency and C_{BV} is a nondimensional coefficient. Equation (24) is not useful in models unless σ_w is available. A second version of this length corresponds to replacing σ_w with the local value of $u_*(z)$ so that

$$l = C_*\frac{u_*(z)}{N}, \quad (25)$$

where C_* is a nondimensional coefficient. The utility of the above z-less formulations is examined in section 6.

4. Observed mixing length

Given observations of the mean shear and momentum flux, the mixing length has been computed from Eq. (8). The various mixing-length formulations are first examined in terms of the fluxes measured at the 40-m level. This level is often above the boundary layer but not too close to the tower top where estimates of vertical gradients of potential temperature and momentum are less reliable. Discrimination between relationships is easier in the upper part of the tower layer where the various formulations do not perform as well compared to those closer to the surface. The poorer performance at higher levels may be partly due to larger eddies and longer adjustment timescale.

The mixing length systematically decreases with increasing nondimensional stability parameters (Figs. 2a–b). The relationship of the mixing length to z/λ (Fig. 2b) shows less scatter compared to the relationship to the Richardson number, partly because of inverse self-correlation due to the fact that the mixing length is proportional to u_* and z/λ is inversely related to u_*^3. Of the various predictors of the mixing length (Figs. 2c–f), the mixing length shows the strongest relationships with $\kappa z/\Phi_m$ and u_*/N, due partly to self-correlation in that both predictors contain u_*. Again, Φ_m is based on local momentum fluxes at level z. Linearly relating the mixing length to $\kappa z/\Phi_m$ at the 40-m level explains 42% of the variance of the mixing length, of which 7% is due to self-correlation. That is, using random data, the variation of $\kappa z/\Phi_m$ explains only 7% of the variance of the mixing length, even though the mixing length and $\kappa z/\Phi_m$ are both proportional to the momentum flux. The spurious self-correlation does not dominate because of the ''relatively'' small variation of surface friction velocity compared to the wind shear. Linear models based on σ_w/N and u_*/N explain 73% and 87% of the variance, respectively, with 0% and 17% of the variance explained caused by self-correlation. The model based on the shear length scale explains only 15% of the variance at this level.

At levels below 40 m, the variance explained increases substantially, ranging from 75%–90% for the similarity prediction $\kappa z/\Phi_m$, 76%–94% for u_*/N, 77%–92% for σ_w/N, and 36%–56% for the shear length scale. However, near the surface, more than half of the variance explained by u_*/N is due to self-correlation. The reason for the generally better performance of the models closer to the surface is not understood, although the relationship of the nondimensional shear to z/λ (Fig. 1) in general tends to degrade somewhat for large values of z/λ, which are more often found at higher levels. The relationships of the mixing length to the Richardson number and the shear length scale exhibit more scatter compared to the other predictors in Fig. 2. Both the Richardson number and the shear length scale involve ratios of gradients, which may be more vulnerable to observational errors.

The present data indicate two advantages for the hybrid similarity theory: the observed mixing length tends to be linearly proportional to $\kappa z/\Phi_m$ and, more importantly, $\kappa z/\Phi_m$ captures most of the height dependence of the mixing length. The other formulations require a coefficient, which depends strongly on height above ground near the surface or requires matching to a surface-based similarity theory near the surface. We first analyze the hybrid similarity prediction $\kappa z/\Phi_m$ in more detail.

5. Hybrid similarity theory

The hybrid similarity prediction $\kappa z/\Phi_m$ captures most of the vertical variation of the mixing length so that no adjustment is required for height; that is, the observed

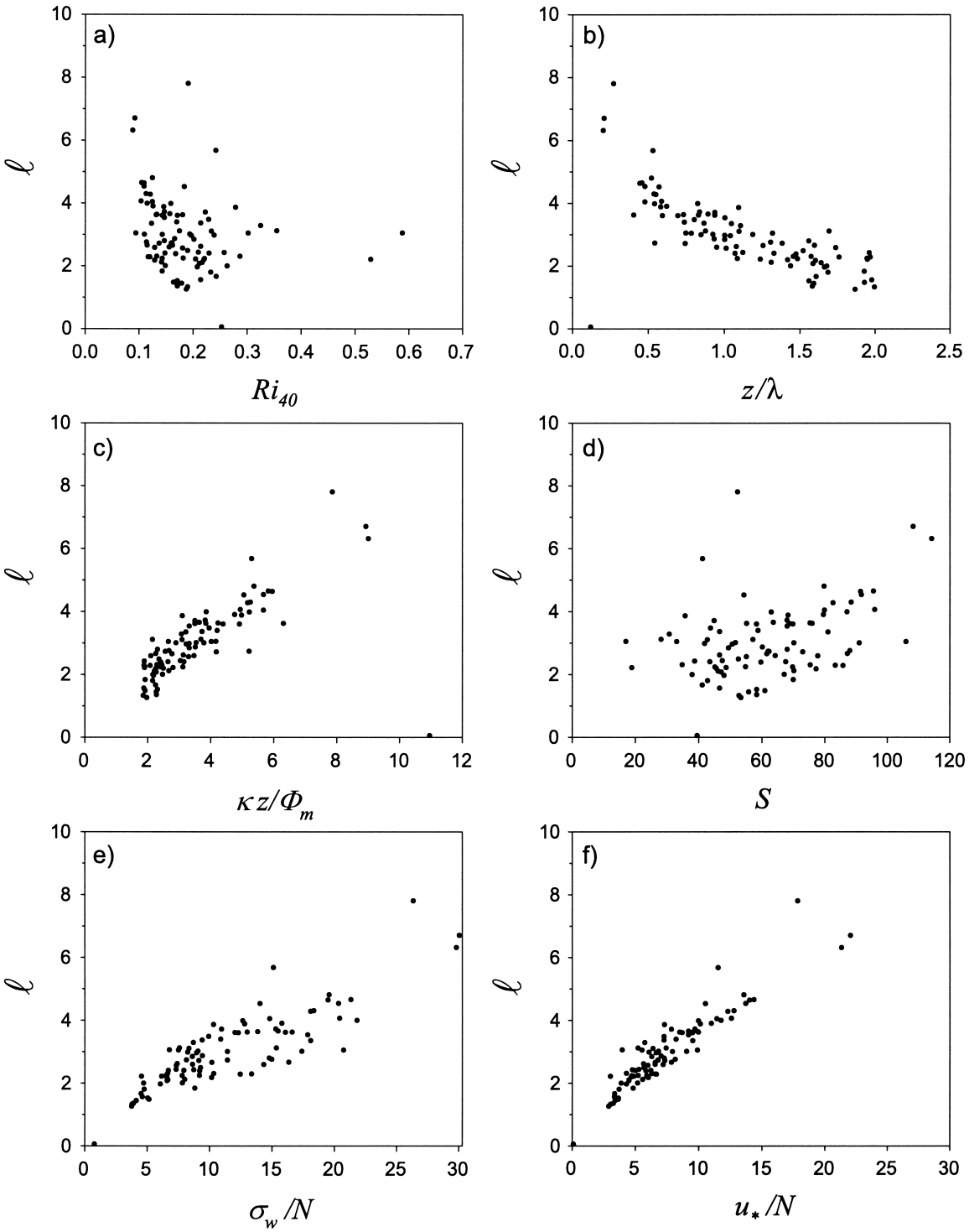

FIG. 2. The relationship between the observed mixing length and (a) a bulk Richardson number, (b) z/λ, (c) the hybrid similarity prediction $\kappa z/\Phi_m$, (d) the shear length scale [Eq. (23)], (e) σ_w/N, and (f) u_*/N for the 40-m level.

mixing length from different heights tends to collapse along the same line (Fig. 3) with relatively small scatter. This collapse does not occur with the other z-less relationships. Part of the success of $\kappa z/\Phi_m$ is due to its limiting behavior of surface layer similarity theory near the surface and its z-less behavior for large z/λ. At $z/\lambda = 2$, the difference between Eq. (18) and the z-less prediction [Eq. (15)] has decreased to about 10%.

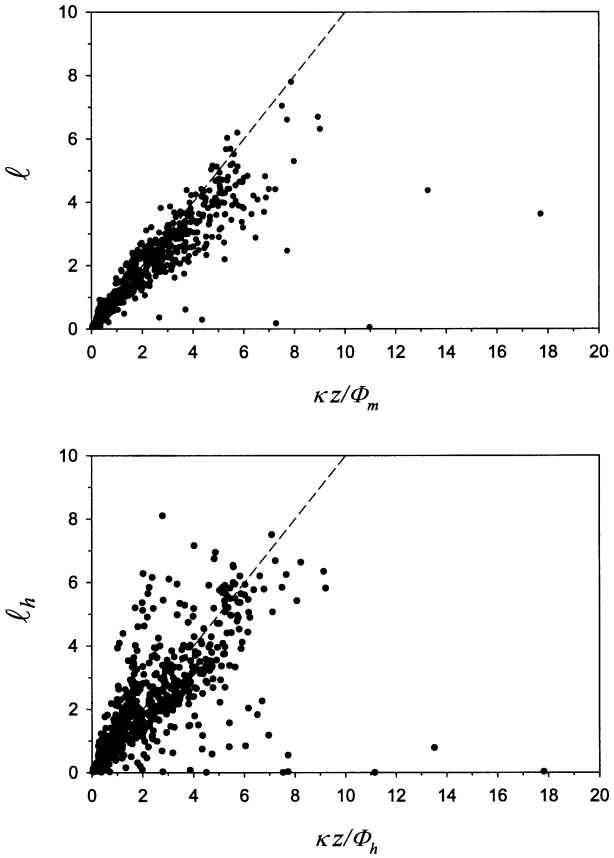

FIG. 3. Relationship between the observed mixing length for (a) momentum and (b) heat, and the hybrid similarity prediction (*x* axis) for all of the levels combined. The dashed line denotes the 1:1 relationship.

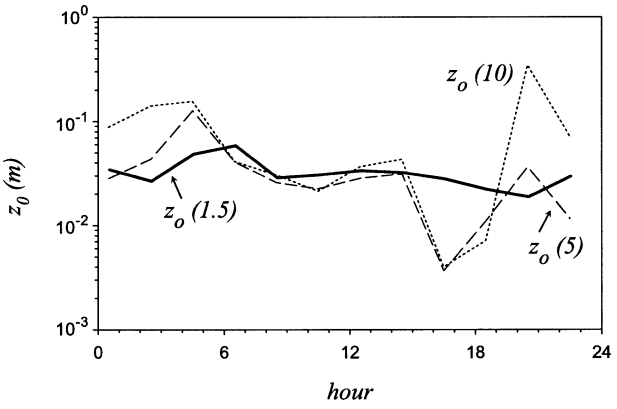

FIG. 4. The dependence of the composited momentum roughness length on time of day for the 1.5-, 5-, and 10-m levels.

a. Small z limit

In the limit of small *z*, where the local fluxes are close to surface values, hybrid similarity theory approaches the Monin–Obukhov similarity theory. For most of the present data, expressing Eq. (4) in terms of surface fluxes instead of local fluxes reduces the performance of the prediction of the mixing length, especially at higher levels. Boundary layer depths are often less than 20 m, in which case surface layer similarity theory is technically valid only in the lowest few meters. With poorly defined boundary layers, fluxes at higher levels are also not well correlated with surface fluxes. The failure of similarity theory at levels as low as 5 m is indicated by the composited diurnal variation of the aerodynamic roughness length (Fig. 4). The roughness length was computed using the Monin–Obukhov similarity theory and the observed heat and momentum fluxes. At 1.5 m, the roughness length for momentum is approximately independent of the time of day. However, for the 5- and 10-m levels, the aerodynamic roughness length is more variable and unrealistically large at night. Since the physical roughness of the surface does not change, this variation must be due to inapplicability of surface layer similarity theory. As a consequence, the study of the surface layer similarity theory requires eddy correlation measurements within the lowest few meters. As an aside, the thermal roughness length varies erratically even at 1.5 m over this simple surface, as found by Sun (1999) over a similar simple grassland.

b. Influence of boundary layer depth

The formulation $\kappa z/\Phi_m$ exhibits a tendency to overestimate the mixing length at higher levels for cases of large $\kappa z/\Phi_m$, possibly due to constraints by the boundary layer depth in some cases. This formulation does not apply to the near-neutral boundary layer ($\Phi \approx 1$), where the observed mixing length is expected to reach a maximum in the interior of the boundary layer and then decrease with height, becoming small near the boundary layer top. The mixing length is constrained by the boundary layer depth and presumably a function of z/h. To include the influence of boundary layer depth for neutral conditions but to reduce its influence for stable conditions, the similarity prediction [Eq. (18)] can be combined with the mixing-length formulation based on the boundary layer depth [Eq. (13)] with the format

$$l = \frac{\kappa z}{\Phi_m}\left(1 - \frac{1}{\Phi_m}\frac{z}{h}\right)^p, \tag{26}$$

where again Φ_m is the local nondimensional shear based on the local momentum flux at level *z*. For the present data, $p \approx 1.5$ provides a reasonable fit to the data although the lack of sensitivity of the overall model performance to the value of *p* does not allow a well-defined determination. When Φ_m becomes large (stable conditions), this relationship approaches the similarity prediction $\kappa z/\Phi_m$, which performed well for all levels in the above analysis. When conditions approach neutral stability ($\Phi_m \approx 1$), the above relationship approaches the mixing length based on boundary layer depth [Eq. (13)]. The tower does not allow evaluation of the mixing

length across the near-neutral or heated boundary layers, which are normally much deeper than the tower.

For stable conditions, boundary layer similarity theory [Eq. (13)] can be applied only to those cases where a definable boundary layer is established. However, the boundary layer depth is always available in most models or can be added with additional parameterization. Any improvement of Eq. (26) over the simpler formulation $\kappa z/\Phi_m$ appears to be insignificant for the present data for stable conditions. The inclusion of boundary layer depth in Eq. (26) does allow what is thought to be proper behavior in the neutral case while having little effect on the significantly stable conditions.

For unstable conditions, where Φ_m becomes less than unity, the modulation of z/h by $1/\Phi_m$ in Eq. (26) leads to overestimation of the mixing length and

$$l = \frac{\kappa z}{\Phi_m}\left(1 - \frac{z}{h}\right)^p \tag{27}$$

becomes a better approximation.

6. Pure *z*-less predictions

a. Richardson number

The observed mixing length is reasonably well related to the gradient Richardson number at all of the tower levels. Several features transcend the behavior of the mixing length at all levels, whether it is within the boundary layer or above it. The mixing length decreases sharply from near-neutral conditions (Ri $\approx$ 0) to modestly stable conditions (Ri $\approx$ 0.20). This decrease is rather systematic considering the large random flux errors and difficulties of estimating mean vertical gradients (section 2). For stronger stability (Ri $>$ 0.20), the value of the mixing length tends to become independent of the Richardson number with large scatter.

To model the *z*-less mixing length based in terms of the Richardson number, we pursue a simple dependence on the form

$$l(z) = l_0(z)\exp(-a\mathrm{Ri}) + b, \tag{28}$$

which becomes *z*-less if l_0 becomes independent of height. The length scale b allows for some residual turbulence at large Richardson numbers, which may be particularly useful for application to grid-averaged fluxes where some turbulence may occur in the grid area, regardless of the magnitude of the Richardson number computed from grid-averaged variables. Based on the present data, we nominally recommend $b = 0.5$ m, although this residual mixing length appears to increase with height. Savijärvi and Kauhanen (2002) found simulation of the very stable boundary layer to be improved by specifying a minimum background turbulence although the results were sensitive to the numerical value of this specification.

The parameter a for the present data is approximately 0.18 and is not particularly sensitive to height. This approach is simpler than that of Kim and Mahrt (1992) and seems to adequately approximate the present data. The principal closure problem is specification of the mixing length at neutral stability l_0. As an adequate approximation for the present data, the neutral mixing length increases linearly with height to a value of 8 m at the 20-m level, and then is approximately independent of height above 20 m. The increase of the near-neutral mixing length with height is approximately κz, although this agreement with κz might be fortuitous. The generality of the 8-m asymptotic value is not known and the specification of a dimensional quantity is unappealing.

b. The shear length scale and buoyancy-based length scales

A nonlinear function of the shear length scale [Eq. (23)] is required for an optimum fit to the data. A linear relationship is useful if one neglects the near-neutral cases. For the linear relationship, the coefficient $C(z)$ is typically about 1.5×10^{-2} but varies somewhat erratically with height. The disadvantage of this approach is that the prediction asymptotes to infinity at neutral conditions where $\Delta\Theta$ vanishes, at least for a fixed Δz. However, with increasing mixing length, the relevant potential temperature difference needs to be computed over a larger vertical scale. For modeling applications, continuous adjustment of the depth over which the gradient is computed may not be practical.

The *z*-less predictions, σ_w/N and u_*/N, also require determination of nondimensional coefficients. For much of the data,

$$l = 0.25\sigma_w/N \tag{29}$$

is a good approximation. The main exception is near the surface where the increase of the mixing length with increasing σ_w/N becomes nonlinear, increasing at a slower rate for large values of σ_w/N.

The relationship

$$l = 0.5u_*/N \tag{30}$$

is also a reasonable approximation, except near the surface where the rate of increase of the mixing length with increasing u_*/N decreases with larger values of u_*/N. Forming nonlinear relationships near the surface is not very appealing because the dimensionality is no longer strictly correct.

Constructing a general formulation of the mixing length from the above pure *z*-less relationships either requires height-dependent coefficients near the surface or some sort of matching with surface layer similarity theory. Simple pseudomatching will take the form

$$\frac{1}{l_s} = \frac{1}{l_b} + \frac{\phi_m}{\kappa z}, \tag{31}$$

where l_b is one of the *z*-less predictions in this section

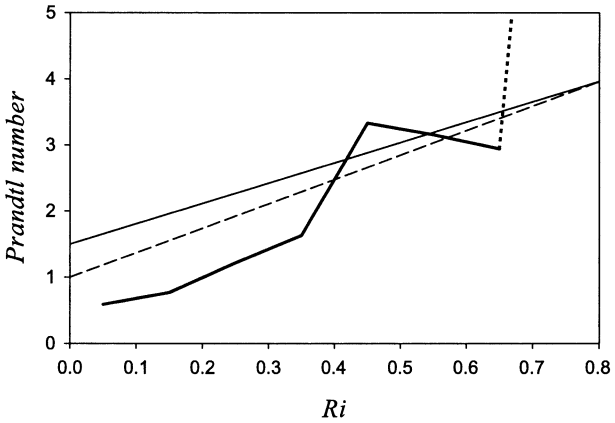

FIG. 5. The Prandtl number based on bin-averaged values of the mixing lengths for intervals of the Richardson number, as a function of the Richardson number for all levels combined. For the largest Richardson numbers, the averaged Prandtl number increases dramatically, although flux sampling errors are probably large. Also shown are the relationship from Kim and Mahrt (solid straight line) and Pr = 1.0 + 3.7 Ri (dashed line).

and ϕ_m is based on the surface fluxes. An alternative algebraic form can be written as

$$l_s = \frac{1}{(1/l_b) + (\phi_m/\kappa z)}. \tag{32}$$

With these formulations, the mixing length is constrained by either stratification or the ground surface, depending on which is more dominant. A dependence on boundary layer depth can be incorporated in the same manner as in section 5 so that

$$l = l_s\left(1 - \frac{1}{\Phi_m}\frac{z}{h}\right)^p. \tag{33}$$

Equations (31)–(33) are more cumbersome than Eq. (26) and no more successful. Data over the entire boundary layer for near-neutral conditions is required for definitive evaluation.

7. Heat transfer

The mixing length for heat shows similar behavior to that for momentum with two exceptions. It generally exhibits more scatter (Fig. 3) and it decreases more rapidly with increasing stability. In strongly stratified flow, the eddy diffusivity for momentum may be larger than that for heat due to momentum transfer by nonlinear gravity waves (e.g., Monti et al. 2002). Based on several datasets, Kim and Mahrt (1992) have formulated this dependence as

$$\frac{K_m}{K_h} = \frac{l_m^2}{l_h^2} = \mathrm{Pr} = 1.5 + 3.08\mathrm{Ri}. \tag{34}$$

The present data also show a similar rapid increase of the Prandtl number with increasing Richardson number to values around 3 for a Richardson number of about 0.5 (Fig. 5). The scatter is large, partly because of errors in the computation of the gradients, which strongly contaminate the computed Richardson number. In Kim and Mahrt, the neutral value of 1.5 was determined to provide the best overall fit for the stable region rather than correctly modeling the neutral limit. In fact, the present data suggest that the neutral limit is less than unity, approximately 0.6, although we do not trust the estimate of the vertical gradient of potential temperature in near neutral conditions (section 2). We suggest a new formulation by conservatively choosing the neutral Prandtl number to be unity (Fig. 5) so that

$$\mathrm{Pr} = 1.0 + 3.7\mathrm{Ri}. \tag{35}$$

The dependence of the Prandtl number on the Richardson number is not compatible with existing Monin–Obukhov similarity and, if real, could explain some of the scatter in the analyses in preceding sections. However, definite conclusions are not possible because of the difficulty of estimating vertical gradients and diffusivities.

8. Conclusions

The mixing lengths for heat and momentum are computed from seven levels of eddy correlation data during CASES-99. Of the various formulations of the mixing length, the hybrid similarity theory relationship $\kappa z/\Phi_m$ performed best in that additional height dependent coefficients were not required and the relationship between the observed mixing length and the hybrid similarity length scale was linear at all levels. Here, Φ_m is based on local fluxes and not surface values. This formulation approaches Monin–Obukhov similarity theory near the surface and approaches a *z*-less prediction at higher levels. A generalized version of this hybrid mixing length [Eq. (26)] includes a dependence on boundary layer depth, which approaches the usual boundary layer height dependence for neutral conditions. However, for many of the observed stable cases, a boundary layer did not exist in the usual sense, in that turbulence was generated primarily above the surface inversion layer and intermittently diffused down to the surface. In the generalized formulation of the mixing length, the role of the boundary layer depth vanishes with strong stability. The formulation for heat flux incorporates the observed rapid increase of the Prandtl number with increasing stability.

The above study also examined the performance of other *z*-less predictions of the mixing length based on the Richardson number, the shear length scale and two length scales based on the buoyancy frequency. The mixing length was roughly linearly related to these predictors above the lowest 20 m, but near the surface, the relationships become more nonlinear, causing dimensional problems. Testing the formulations developed in this study within a numerical model is beyond the scope of the study. However, the performance of such formulations is expected to depend on the details of the

host model, such as inclusion of radiative flux divergence and preexisting specification of criteria to control runaway surface cooling (Delage et al. 2002).

Acknowledgments. We gratefully acknowledge the field assistance of the NCAR ATD staff, Jielun Sun and Sean Burns and the extensive useful comments of Don Lenschow. This material is based upon work supported by Grant DAAD 19-0210224 from the Army Research Office and Grant 0107617-ATM from the Physical Meteorology Program of the National Sciences Program.

REFERENCES

Arya, S. P., 1998: *Introduction to Micrometeorology.* Academic Press, 420 pp.

Ballard, S. P., B. W. Golding, and R. N. B. Smith, 1991: Mesoscale model experimental forecasts of the Haar of northeast Scotland. *Mon. Wea. Rev.,* **119,** 2107–2123.

Beljaars, A. C. M., and A. A. M. Holtslag, 1991: Flux parameterization over land surfaces for atmospheric models. *J. Appl. Meteor.,* **30,** 327–341.

Beyrich, F., 1997: Mixing height estimation from sodar—A critical discussion. *Atmos. Environ.,* **21,** 3941–3953.

Blackadar, A. K., 1957: Boundary layer wind maxima and their significance for the growth of nocturnal inversions. *Bull. Amer. Meteor. Soc.,* **38,** 283–290.

——, 1962: The vertical distribution of wind and turbulent exchange in a neutral atmosphere. *J. Geophys. Res.,* **67,** 3095–3102.

Brost, R. A., and J. C. Wyngaard, 1978: A model study of the stably stratified planetary boundary layer. *J. Atmos. Sci.,* **35,** 1427–1440.

Burns, S., J. Sun, A. C. Delany, T. W. Horst, and S. P. Oncley, 2003: A field intercomparison technique to improve the relative accuracy of longwave radiation measurements and an evaluation of CASES-99 pyrgeometer data quality. *J. Atmos Oceanic Technol.,* **20,** 348–361.

Chimonas, G., 2002: On internal gravity waves associated with the stable boundary layer. *Bound.-Layer Meteor.,* **102,** 139–155.

Cuxart, J. C., and Coauthors, 2000: Stable Atmospheric Boundary-Layer Experiment in Spain (SABLE 98): A report. *Bound.-Layer Meteor.,* **96,** 337–370.

Delage, Y., 1974: A numerical study of the nocturnal atmospheric boundary layer. *Quart. J. Roy. Meteor. Soc.,* **100,** 351–364.

——, P. A. Bartlett, and J. H. McCaughey, 2002: Study of ''soft'' night-time surface-layer decoupling over forest canopies in a land surface model. *Bound.-Layer Meteor.,* **103,** 253–276.

Derbyshire, S., 1999: Boundary-layer decoupling over cold surfaces as a physical boundary-instability. *Bound.-Layer Meteor.,* **90,** 297–325.

Dyer, A. J., 1974: A review of flux-profile relationships. *Bound.-Layer Meteor.,* **7,** 363–372.

Garratt, J. R., 1992: *The Atmospheric Boundary Layer.* Cambridge University Press, 316 pp.

Ha, K.-J., and L. Mahrt, 2001: Simple inclusion of *z*-less turbulence within and above the modeled nocturnal boundary layer. *Mon. Wea. Rev.,* **129,** 2136–2143.

Hicks, B. B., 1978: Some limitations of dimensional analysis and power laws. *Bound.-Layer Meteor.,* **14,** 567–569.

Högström, U., 1996: Review of some basic characteristics of the atmospheric surface layer. *Bound.-Layer Meteor.,* **78,** 215–246.

Kim, J., and L. Mahrt, 1992: Simple formulation of turbulent mixing in the stable free atmosphere and nocturnal boundary layer. *Tellus,* **44A,** 381–394.

Mahrt, L., 1999: Stratified atmospheric boundary layers. *Bound.-Layer Meteor.,* **90,** 375–396.

——, and D. Vickers, 2002: Contrasting vertical structures of nocturnal boundary layers. *Bound.-Layer Meteor.,* **105,** 351–363.

Monin, A. S., and A. M. Obukhov, 1954: Basic laws of turbulent mixing in the atmosphere near the ground. *Tr. Akad. Nauk SSSR Geofiz. Inst.,* **24,** 163–187.

——, and A. M. Yaglom, 1971: *Statistical Fluid Mechanics.* Vol. 1., *Mechanics of Turbulence,* MIT Press, 769 pp.

Monti, P., H. J. S. Fernando, M. Princevac, W. C. Chan, T. A. Kowalewski, and E. R. Pardyjak, 2002: Observations of flow and turbulence in the nocturnal boundary layer over a slope. *J. Atmos. Sci.,* **59,** 2513–2534.

Nappo, C. J., 1991: Sporadic breakdown of stability in the PBL over simple and complex terrain. *Bound.-Layer Meteor.,* **54,** 69–87.

Nieuwstadt, F. T. M., 1984: The turbulent structure of the stable, nocturnal boundary layer. *J. Atmos. Sci.,* **41,** 2202–2216.

Ohya, Y., 2001: Wind-tunnel study of atmospheric stable boundary layers over a rough surface. *Bound.-Layer Meteor.,* **98,** 57–82.

Ostdiek, V., and W. Blumen, 1997: A dynamic trio: Inertial oscillation, deformation frontogenesis, and the Ekman–Taylor boundary layer. *J. Atmos. Sci.,* **54,** 1490–1502.

Poulos, G. S., and Coauthors, 2002: CASES-99: A comprehensive investigation of the stable nocturnal boundary layer. *Bull. Amer. Meteor. Soc.,* **83,** 757–779.

Raupach, M. R., 1994: Simplified expressions for vegetation roughness length and zero-plane displacement as functions of canopy height and area index. *Bound.-Layer Meteor.,* **71,** 211–216.

Savijärvi, H., and J. Kauhanen, 2002: High resolution numerical simulations of temporal and vertical variability in the stable wintertime boreal boundary layer: A case study. *Theor. Appl. Climatol.,* **70,** 97–103.

Smedman, A.-S., 1988: Observations of a multi-level turbulence structure in a very stable atmospheric boundary layer. *Bound.-Layer Meteor.,* **44,** 231–253.

——, H. Tjernström, and U. Högström, 1993: Analysis of the turbulence structure of a marine low-level jet. *Bound.-Layer Meteor.,* **66,** 105–126.

Sorbjan, Z., 1986: On similarity in the atmospheric boundary layer. *Bound.-Layer Meteor.,* **34,** 377–398.

——, 1988: Structure of the stably-stratified boundary layer during the SESAME-1979 experiment. *Bound.-Layer Meteor.,* **44,** 255–266.

——, 1989: *Structure of the Atmospheric Boundary Layer.* Prentice Hall, 317 pp.

Stull, R. B., 1990: *An Introduction to Boundary Layer Meteorology.* Kluwer Academic, 666 pp.

Sun, J., 1999: Diurnal variation of thermal roughness height over a grassland. *Bound.-Layer Meteor.,* **92,** 407–427.

——, and Coauthors, 2003: Intermittent turbulence associated with a density current passage in the stable boundary layer. *Bound.-Layer Meteor.,* **105,** 199–219.

Therry, G., and P. Lacarrere, 1983: Improving the eddy kinetic energy model for p.b.l. description. *Bound.-Layer Meteor.,* **25,** 63–88.

Troen, I., and L. Mahrt, 1986: A simple model of the atmospheric boundary layer: Sensitivity to surface evaporation. *Bound.-Layer Meteor.,* **37,** 129–148.

Vickers, D., and L. Mahrt, 1997: Quality control and flux sampling problems for tower and aircraft data. *J. Atmos. Oceanic Technol.,* **14,** 512–526.

——, and ——, 1999: Observations of nondimensional shear in the coastal zone. *Quart. J. Roy. Meteor. Soc.,* **125,** 2685–2702.

——, and ——, 2003: The cospectral gap and turbulent flux calculations. *J. Atmos. Oceanic Technol.,* **20,** 660–672.

Wyngaard, J. C., 1973: On surface-layer turbulence. *Workshop on Micrometeorology,* D. A. Haugen, Ed., Amer. Meteor. Soc., 101–149.

Zilitinkevich, S., and D. Mironov, 1996: A multi-limit formulation for the equilibrium depth of a stably stratified boundary layer. *Bound.-Layer Meteor.,* **81,** 325–351.